AMERICAN SOCIETY FOR MICROBIOLOGY | Journal of Virology

Correlation between Virus Replication and Antibody Responses in Macaques following Infection with Pandemic Influenza A Virus

Gerrit Koopman,[a] Petra Mooij,[a] Liesbeth Dekking,[b] Daniëlla Mortier,[a] Ivonne G. Nieuwenhuis,[a] Melanie van Heteren,[a]* Harmjan Kuipers,[b] Edmond J. Remarque,[c] Katarina Radošević,[b]* Willy M. J. M. Bogers[a]

Department of Virology[a] and Department of Parasitology,[c] Biomedical Primate Research Centre, Rijswijk, The Netherlands; Crucell Holland B.V., Janssen Pharmaceutical Companies of Johnson & Johnson, Leiden, The Netherlands[b]

ABSTRACT

Influenza virus infection of nonhuman primates is a well-established animal model for studying pathogenesis and for evaluating prophylactic and therapeutic intervention strategies. However, usually a standard dose is used for the infection, and there is no information on the relation between challenge dose and virus replication or the induction of immune responses. Such information is also very scarce for humans and largely confined to evaluation of attenuated virus strains. Here, we have compared the effect of a commonly used dose (4×10^6 50% tissue culture infective doses) versus a 100-fold-higher dose, administered by intrabronchial installation, to two groups of 6 cynomolgus macaques. Animals infected with the high virus dose showed more fever and had higher peak levels of gamma interferon in the blood. However, virus replication in the trachea was not significantly different between the groups, although in 2 out of 6 animals from the high-dose group it was present at higher levels and for a longer duration. The virus-specific antibody response was not significantly different between the groups. However, antibody enzyme-linked immunosorbent assay, virus neutralization, and hemagglutination inhibition antibody titers correlated with cumulative virus production in the trachea. In conclusion, using influenza virus infection in cynomolgus macaques as a model, we demonstrated a relationship between the level of virus production upon infection and induction of functional antibody responses against the virus.

IMPORTANCE

There is only very limited information on the effect of virus inoculation dose on the level of virus production and the induction of adaptive immune responses in humans or nonhuman primates. We found only a marginal and variable effect of virus dose on virus production in the trachea but a significant effect on body temperature. The induction of functional antibody responses, including virus neutralization titer, hemagglutination inhibition titer, and antibody-dependent cell-mediated cytotoxicity, correlated with the level of virus replication measured in the trachea. The study reveals a relationship between virus production and functional antibody formation, which could be relevant in defining appropriate criteria for new influenza virus vaccine candidates.

Nonhuman primates (NHP) play an important role as animal models for influenza virus research (1, 2). Novel candidate influenza vaccines are commonly tested for safety and efficacy in mice and ferrets and/or macaques before they are evaluated for immunogenicity in humans (2, 3). However, whereas for mice and ferrets dose-finding studies have been described and implemented for testing of vaccines and antiviral agents (4–11), for macaques usually a standard challenge dose is used, typically in the range between 10^6 and 10^7 50% tissue culture infective doses ($TCID_{50}$) (12–15).

Information from human volunteer challenge studies on the effect of influenza virus infection dose on viral replication and induced adaptive immunity is limited, because dose escalation is usually performed for attenuated viruses that are to be used as a vaccine modality (16–21) and only occasionally for the wild-type virus (18, 22, 23). In general, the studies with attenuated viruses have shown that an increase in challenge dose results in increased virus shedding (18–20). However, reports differ in their conclusions on the effect of challenge dose and levels of virus production on the induction of antiviral and hemagglutination-inhibitory (HAI) antibody (Ab) responses (17–21). Dose finding in mice and ferrets is mostly directed at defining the minimal infectious dose to be used to obtain pathology or lethal infection and not particularly at the effect on virus production or induction of immune responses.

The dose-finding studies are commonly not performed in NHP, and only a few studies have addressed the induction of adaptive immune responses after viral challenge in macaques (24–26). No correlation was drawn between levels of virus production and strength or neutralizing capacity of the induced antibody responses. In this study, we evaluated effects of two different chal-

Received 28 October 2015 **Accepted** 29 October 2015

Accepted manuscript posted online 4 November 2015

Citation Koopman G, Mooij P, Dekking L, Mortier D, Nieuwenhuis IG, van Heteren M, Kuipers H, Remarque EJ, Radošević K, Bogers WMJM. 2016. Correlation between virus replication and antibody responses in macaques following infection with pandemic influenza A virus. J Virol 90:1023–1033. doi:10.1128/JVI.02757-15.

Editor: S. Schultz-Cherry

Address correspondence to Petra Mooij, mooij@bprc.nl.

* Present address: Melanie van Heteren, Infectious Diseases and Vaccines Therapeutic Area, Janssen Research and Development, Pharmaceutical Companies of Johnson and Johnson, Leiden, The Netherlands; Katarina Radošević, Sanofi, Global Biotherapeutics, Vitry-sur-Seine, France.

lenge doses on symptom development, virus production, body temperature, and antibody response. We chose to compare the effects of a controlled intrabronchial inoculation of a standard dose of influenza virus of 10^6 $TCID_{50}$, with a high dose of virus of 10^8 $TCID_{50}$, in an attempt to develop a more robust and uniform challenge model by increasing the clinical manifestations in the majority of the animals, such as sneezing and coughing, thereby disseminating the virus to the upper respiratory tract. This would facilitate the evaluation of vaccine efficacy, reducing the number of animals needed per group, but risking the possibility of making the model too stringent to show protection from infection. We demonstrated no effect of the dose on virus production but a significant effect on the body temperature. In addition, the variation in the obtained virus titers allowed us to identify a correlation between virus replication and induction of virus binding and neutralizing antibody (NAb) responses and antibodies mediating antibody-dependent cell-mediated cytotoxicity (ADCC).

MATERIALS AND METHODS

Animals, housing, and clinical observation. This study was performed in outbred male mature Malaysian origin cynomolgus monkeys (*Macaca fascicularis*). Animals were captive bred for research purposes and socially housed at animal biosafety level III facilities at the Biomedical Primate Research Center, Rijswijk, The Netherlands (an AAALAC-accredited institution). Animal housing was according to international guidelines for nonhuman primate care and use (European Council Directive 86/609/EEC and Convention ETS 123, including the revised Appendix A as well the Standard for Humane Care and Use of Laboratory Animals by Foreign institutions, identification number A5539-01, provided by the Department of Health and Human Services of the U.S. National Institutes of Health [NIH]). All animal handling was performed at the Department of Animal Science (ASD) according to Dutch law. A large, experienced staff was available, including full-time veterinarians and a pathologist. ASD is regularly inspected by the responsible authority (Voedsel en Waren Autoriteit [VWA]) and by an independent animal welfare officer. The animals were negative for antibodies to simian type D retrovirus or simian T-cell lymphotropic virus and were selected for absence of antibodies directed against conserved nucleo- and matrix proteins covering all human and avian influenza A and B viruses (Serion enzyme-linked immunosorbent assay [ELISA] classic influenza A/B virus IgA/IgG/IgM detection kit [ESR 1231; Serion Immunodiagnostica GmbH, Würzburg, Germany]) and to influenza A/PR/8/34 (H1N1) viral lysate (Advanced Biotechnologies Inc., Eldersburg, MD, USA). All animals were classified healthy according to physical examination and evaluation of complete blood count and serum chemistry.

During the experiment the animals were housed in pairs with a socially compatible cage mate. Animals were kept on a 12-hour light/dark cycle and were housed in a single room separated from the rest of the colony. The monkeys were offered a daily diet consisting of monkey food pellets (Hope Farms, Woerden, The Netherlands), fruit, and bread. Enrichment was provided daily in the form of pieces of wood, mirrors, food puzzles, and a variety of other homemade or commercially available enrichment products. Drinking water was available *ad libitum* via an automatic watering system. Veterinary staff provided daily health checks before infection, and the animals were checked for appetite, general behavior, and stool consistency. During the course of the influenza virus infection, the animals were checked twice a day and scored for clinical symptoms according to a previously published scoring system (27), with scores for changes such as skin and fur abnormalities, posture, eye and nasal discharge, sneezing and coughing, and respiration rate. A score of 35 or more was predetermined as an endpoint and justification for euthanasia. Each time an animal was sedated, the body weight was measured. Body temperature was recorded on a data storage tag (DST; Micro-T; Star-Oddi, Iceland) surgically placed in the abdominal cavity of each animal 28 days before infection; the tag recorded body temperature every 15 min. All possible precautions were taken to ensure the welfare of and to avoid any discomfort to the animals. All experimental interventions (intrabronchial infection, swabs, blood samplings) were performed under anesthesia using ketamine (10 mg/kg of body weight).

The Institutional Animal Care and Use Committee of the Biomedical Primate Research Centre (dierexperimentencommissie; DEC-BPRC) approved the study protocols, which were developed according to strict international ethical and scientific standards and guidelines. The qualifications of the members of this committee, including their independence from a research institute, is requested in Dutch law for animal experiments (1996 Wet op de Dierproeven).

Experimental infection and influenza virus replication. Six male adult cynomolgus monkeys were experimentally inoculated with 4×10^6 $TCID_{50}$ of an influenza A/Mexico/InDRE4487/2009 (H1N1) (Mex4487) virus stock that was produced on Madin-Darby canine kidney (MDCK) cells. Another six male adult cynomolgus monkeys were experimentally inoculated with a 100-fold-higher virus dose, that is, 4×10^8 $TCID_{50}$ of H1N1 influenza A Mex4487 virus. This virus was originally isolated from the bronchial aspirate of a 26-year-old man from a family cluster of three confirmed severe flu cases in Mexico (28). Infection was performed as previously described (29) via the intrabronchial route using a bronchoscope. The intrabronchial route of infection is very controlled in terms of the amount of virus deposition and location. A 2-ml aliquot of a virus suspension containing either 10^6 or 10^8 $TCID_{50}$/ml was administered in each bronchus.

During the infection procedure, animals were sedated with ketamine (10 mg/kg). Additionally, they received medetomidine hydrochoride (0.04 mg/kg; Cepetor) to induce further sedation and muscle relaxation. At the end of the procedure, atipamezole hydrochloride (0.5 mg/kg; Revertor) was used for faster recovery. Local anesthesia in the throat was applied by spraying with 10% xylocaine (lidocaine).

Blood, tracheal, and nasal swabs were collected on days 0, 1, 2, 4, 6, 8, 10, 14, and 21. Swabs were taken using flocked swabs (FLOQswabs; catalog number 502CS01; Copan).

Virus replication was monitored in standard $TCID_{50}$ assays on MDCK cells. The detection limit of this assay was 100 infectious viral particles/ml. Viral RNA was detected by real-time PCR, as described previously (30). The dynamic range of the quantitative reverse transcription-PCR (QRT-PCR) assay was 3.5 to 10.5 log RNA copies/ml.

Hematology and assessment of cytokine and chemokine protein levels in serum. Hematology parameters were measured in EDTA-blood mixtures with a Sysmex XT-2000iV automated hematology analyzer (Sysmex Corporation of America) as previously described (31).

Cytokine and chemokine concentrations, including granulocyte colony-stimulating factor (G-CSF), granulocyte-macrophage CSF (GM-CSF), IFN-γ, interleukin-1β (IL-1β), IL-1 receptor antagonist (IL-1Ra), IL-2, IL-4, IL-6, IL-8, IL-12, IL-13, IL-15, IL-17, IL-18, monocyte chemoattractant protein 1 (MCP-1), macrophage inflammatory protein 1α (MIP-1α), MIP-1β, soluble CD40 ligand (sCD40L), transforming growth factor alpha (TGF-α), and tumor necrosis factor alpha (TNF-α), were determined using the Milliplex multianalyte panel (MAP) nonhuman primate cytokine magnetic bead panel kit (Millipore, Billerica, MA, USA) and a Luminex detection system (Luminex Corporation, Austin, TX, USA), according to the manufacturers' instructions. For each cytokine, a standard curve was made, ranging from 2.4 to 10,000 pg/ml. Samples were measured on a Bio-Plex 2000 system (Bio-Rad, Herts, United Kingdom) and analyzed by using Bio-Plex Manager software.

Antibody titers. Serum samples from 8 weeks postinfection were tested for the presence of anti-influenza virus antibodies using an ELISA. Wells of a 96-well microtiter plate (Nunc Maxisorp) were coated overnight at 4°C with 100 μl 1:100-diluted Pandemrix vaccine preparation (split influenza virus, inactivated, containing 7.5 μg hemagglutinin [HA]/ml of the A/California/7/2009 [H1N1] influenza virus strain propagated in eggs, without ASO3 adjuvant). Wells were washed four times

with phosphate-buffered saline (PBS) containing 0.05% (vol/vol) Tween 20 and blocked in PBS containing 1% (wt/vol) bovine serum albumin (BSA; blocking solution) for 1 h at room temperature. Diluted serum (1% BSA in PBS) samples were added and incubated for 1 h at room temperature, and wells were washed four times with PBS–0.05% Tween 20. Bound anti-influenza virus antibodies were detected using alkaline phosphatase-conjugated protein G (Calbiochem EMD, Millipore Corporation USA; 1:100-diluted in PBS) and incubated for 1 h at room temperature. Wells were washed four times with PBS–0.05% Tween 20. The reaction was developed with the BluePhos microwell phosphatase substrate system (Kirkegaard & Perry Laboratories, USA) for 10 min. The absorbance was measured at 595 nm.

Influenza virus neutralization assay. To remove nonspecific inhibitors of agglutination, serum samples from 8 weeks postinfection were treated with RDE (receptor-destroying enzyme). Subsequently, 2-fold serial dilutions of the serum samples were made in a 96-well flat-bottom plate (Nunc). A total of 100 $TCID_{50}$ of MDCK-grown influenza A/Mexico/InDRE4487/2009 (H1N1) was added to each well containing serum and incubated for 2 h at 37°C. The virus-antibody mixtures were transferred to a 96-well microtiter plate with confluent MDCK cells and incubated at 37°C, 5% CO_2, until cytopathic effect (CPE) occurred (3 days). Virus growth and CPE were confirmed with the hemagglutination assay, performed by transferring supernatant to 1% turkey red blood cells (TRBC). After 45 min of incubation at room temperature, agglutination was determined visually. The virus neutralization titer was determined as the inverse of the last serum dilution showing 50% or more CPE or hemagglutination. Samples were tested in duplicate.

HAI assays. Hemagglutination inhibition (HAI) assays were performed on serum samples from 8 weeks postinfection, as described in the 2002 *WHO Manual on Animal Influenza Diagnosis and Surveillance* (32). To remove nonspecific inhibitors of agglutination, serum samples were treated with RDE and subsequently washed with 1% TRBC in PBS. HAI assays were performed by standard procedures in 96-well round-bottom microtiter plates (Nunc) using 0.5% TRBC. Twofold serial dilutions from sera were made from a starting dilution of 1:10 to 1:5,120 in PBS solution. Serum dilutions were incubated with 0.5% TRBC for 45 min at room temperature, and agglutination was determined visually. Titers were expressed as the reciprocal of the highest dilution of plasma that completely inhibited 8 hemagglutinating units of influenza A virus strain Mex4487. Samples were tested in duplicate.

Plate-bound antibody-dependent cellular cytotoxicity NK cell activation assay. The ADCC NK cell activation assay was performed as described before (33) with minor modifications. Wells of a 96-well ELISA plate (Maxisorp, Nunc) were coated overnight at 4°C with 400 ng/well purified HA protein (influenza A H1N1 California 04/2009 or Puerto Rico 8/34; Sino Biological Inc., China) in PBS. Wells were washed 3 times with PBS and incubated with diluted (in PBS–1% BSA) heat-inactivated sera (56°C for 60 min) collected at 8 weeks postinfection for 2 h at 37°C. Serum was discarded, and 0.5×10^6 thawed peripheral blood mononuclear cells/well from a healthy macaque in R10 medium (RPMI supplemented with 10% fetal calf serum [FCS], penicillin, streptomycin, and L-glutamine; Gibco, LifeTechnologies) were added. Additionally, anti-human CD107a–allophycocyanin Ab conjugate (H4A3 clone; BD Biosciences, San Jose, CA), 5 mg/ml brefeldin A (GolgiPlug; BD Biosciences), and 5 mg/ml monensin (Golgi Stop; BD Biosciences) were added and incubated for 5 h at 37°C with 5% CO_2. Cells were then transferred to a V-bottom plate (Greiner) and stained with LIVE/DEAD fixable violet dead cell stain (Molecular Probes) for 15 min at room temperature followed by incubation with anti-human CD3–fluorescein isothiocyanate conjugate Ab (clone SP34; BD Biosciences), anti-human CD14–phycoerythrin-Texas Red Ab conjugate (clone RMO52, Beckman Coulter), and anti-human NKG2a–phycoerythrin Ab conjugate (clone Z199; Beckman Coulter) for 30 min at room temperature in the dark. Cells were permeabilized with Perm/Fix solution (BD Biosciences) for 20 min and washed with Perm/Wash solution (BD Biosciences). Finally, cells were incubated at room temperature for 30 min with IFN-γ–AF700 conjugate (clone B27; BD Biosciences). Cells were fixed with 2% paraformaldehyde overnight at 4°C, and acquisition was performed on the LSRII flow cytometer (BD Biosciences) with up to 3×10^5 lymphocyte events collected. Samples were analyzed using FlowJo version 10. For analysis, cells within the lymphocyte gate were selected, and then cells negative for CD3, CD14, and staining with the LIVE/DEAD marker and positive for NKG2A were selected. Within this cell population, defined as NK cells, expression of CD107a was plotted against IFN-γ- and CD107a-positive as well as CD107a/IFN-γ-double-positive cells. To quantify the ADCC-enhancing capacities, sera were tested in a dilution range and the dilution that induced 50% of the plateau ADCC activity level was calculated as the 50% effective concentration (EC_{50}).

Statistical evaluation. Statistical significance of differences between the dose groups was calculated by using the Mann-Whitney test. A two-sided α level of 0.05 was used to determine significance. Correlations between parameters were determined with the Spearman correlation test.

RESULTS

An increased influenza virus inoculation dose does not induce more clinical symptoms. During the course of the influenza virus infection the animals were scored twice a day for clinical symptoms according to a previously published scoring system (27) that included scores for skin and fur abnormalities, posture, eye and nasal discharge, sneezing and coughing, respiration rate, tremor, etc. Only a few clinical symptoms were observed upon influenza virus infection in any of the animals (Fig. 1). Most frequently, a loss of appetite and changes in stool consistency were observed (Fig. 1A), while only 4 animals showed influenza virus infection-related symptoms (Fig. 1B), such as shortness of breath or coughing (animals 5 and 7), hunched posture (animals 7 and 9), untended fur (animals 9 and 12), and tremor (animals 5 and 7). Although the total clinical score did not statistically differ between animals infected with a normal or high influenza virus dose (area under the curve [total clinical score versus time; AUC], 22.2 ± 5.3 versus 22.2 ± 9.3 [mean total score ± SD]), the number of animals showing specific influenza virus-related clinical symptoms was higher in the group infected with a high influenza virus dose (3 out of 6 animals) than in animals that received a normal influenza virus dose (1 out of 6) (Fig. 1B).

Development of earlier and higher fever after infection with the high dose of influenza virus. Body temperature was recorded every 15 min on a data logger (Star-Oddi) surgically implanted in the abdominal cavity of each animal (28 days before infection) and removed at the end of the study. This method of body temperature registration allowed accurate measurements throughout the study period without sedation, and we obtained valuable information that would have otherwise been lost.

Each animal showed a clear circadian body temperature pattern, with lowest temperatures around midnight and highest around 15:00 in the afternoon. The mean 24-h circadian pattern was calculated by taking the mean of the body temperatures recorded at the same time of the day during a period of 3 weeks before infection. In Fig. 2A, the mean recorded preinfection body temperatures, with 95% confidence intervals, are shown in gray. Each animal developed a fever, defined as an increase in temperature above the circadian pattern recorded before infection, which peaked around day 2 after infection (Fig. 2A, in black). Some animals showed a second fever peak around day 7 (animals 5, 6, 8, and 11). The increase in body temperature after infection was significantly higher in cynomolgus macaques who received the

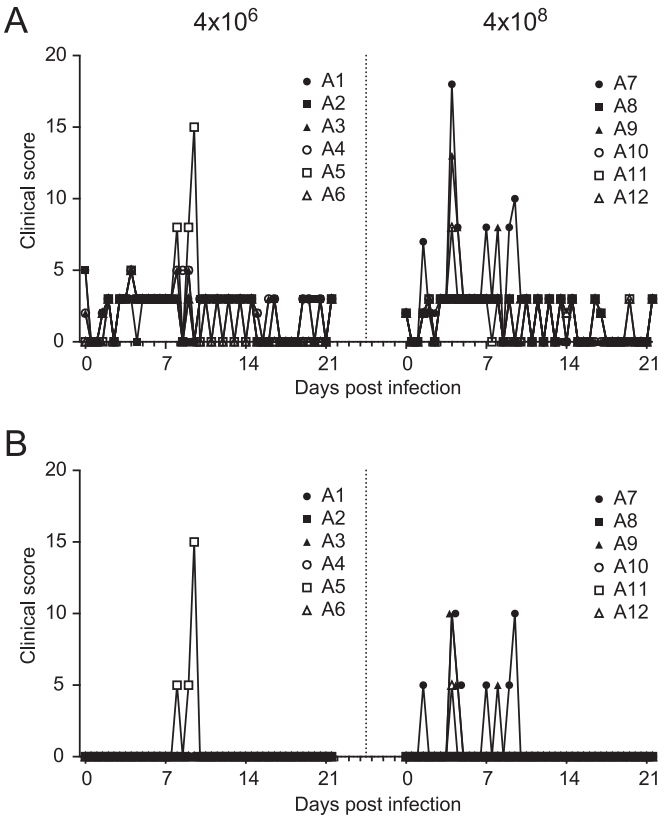

FIG 1 Total clinical scores. (A) The total clinical score over the period of 21 days after infection of animals that received a low-dose challenge (4×10^6 $TCID_{50}$) and animals that received a high-dose challenge (4×10^8 $TCID_{50}$). During the course of the influenza virus infection, the animals were checked twice a day and scored for clinical symptoms according to a previously published scoring system (27) that included changes such as loss of appetite, stool consistency, skin and fur abnormalities, posture, eye and nasal discharge, sneezing and coughing, and respiration rate. (B) Total clinical scores for individual animals after infection, excluding scoring of appetite and stool consistency.

highest influenza virus dose (AUC of net temperature [mean temperature, with the mean circadian temperature plus the upper level of the 95% confidence interval subtracted[) (Fig. 2B) during the first day ($P = 0.008$) and first 3 days after infection ($P = 0.008$). Fever developed directly after infection with a high influenza virus dose, while infection with a low influenza virus dose resulted in delayed fever development by 1 day (Fig. 2A).

The level of virus replication does not correlate with influenza virus inoculation dose. Virus levels, as detected by PCR, were highest in the tracheal swabs and only occasionally detected in nasal swabs (Fig. 3). The total cumulative virus load over time (area under the curve) in the trachea was not significantly different between animals receiving the low or high influenza virus dose, although virus was present at higher levels in 2 out of 6 animals (animals 7 and 12) and for a longer duration in 3 out of 6 animals (animals 7, 10, and 12) that received the high influenza virus inoculation dose.

Early decrease of neutrophilic granulocytes upon infection with a high influenza virus dose. Evaluation of circulating white blood cells upon influenza virus infection revealed a prominent and early decrease in the number of lymphocytes, with the lowest counts reached at day 1 after infection (Fig. 4). This decrease was similar in animals infected with a low or high dose of influenza virus. The absolute number of neutrophilic granulocytes also decreased upon infection, but the decrease was seen earlier in the high-dose than the low-dose group ($P < 0.01$; Mann-Whitney test comparing absolute numbers at day 1 postinfection of both groups). The effect of influenza virus infection dose on the number of circulating monocytes was more complex, with increases and decreases in animals from both groups (Fig. 4).

Cytokine and chemokine expression levels after influenza virus Mex4487 infection. Infection with Mex4487 influenza virus induced increased blood levels of IL-6, MCP-1, IL-15, and IFN-γ (Fig. 5). Animals infected with a high influenza virus dose tended to show higher peak levels of IL-6 ($P = 0.06$) and had significantly higher peak levels of IFN-γ ($P < 0.01$) in the blood than animals infected with a low influenza virus dose. One animal from the high-dose infection group (A11) already showed very high IFN-γ levels before infection (Fig. 5). Even when data from this outlier were excluded, peak levels were still significantly higher in animals infected with a high influenza virus dose than in animals infected with a low influenza virus dose. Levels of IL-8 also increased and peaked (range, 1,350 to 11,000 pg/ml) at 6 days postinfection in the majority of the animals (data not shown), but the changes did not statistically differ between groups. Other cytokines analyzed were either below the detection limit of 2.4 pg/ml (GM-CSF, IL-1β, IL-2, IL-4, IL-13, IL-17, IL-18, MIP-1α, MIP-1β, TNF-α) or were present at levels not affected by the dose of influenza virus inoculation (G-CSF, IL-1Ra, IL-12, sCD40L, TGFα) (data not shown).

Antibody titers correlated with cumulative virus production. All animals developed antibody responses against the homologous influenza California/7/2009 virus by 8 weeks postinfection. In addition to virus binding antibodies, as detected by ELISA (Fig. 6A), all animals also developed influenza virus Mex4487 NAb (Fig. 6B) as well as HAI antibodies (Fig. 6C). There were no significant differences between the groups in any of these antibody responses. Interestingly, the virus-binding, virus-neutralizing, and HAI antibody titers were positively correlated with cumulative virus production (AUC) in the trachea (Fig. 6D to F). The heterologous influenza virus A/Puerto Rico/8/34 (H1N1) strain, for which the HA sequence shows 76 amino acid differences with HA of Mex4487, was not neutralized by any of the postinfection sera (tested at a 1:10 dilution) (data not shown). ADCC was evaluated by measuring expression of CD107a on NK cells, as a measure of NK cell degranulation and activation, after incubation on plate-bound purified influenza virus HA protein in the absence or presence of serum, as recently described as a valid method by Jegaskanda et al. (33). Because we did not have purified HA protein from the Mex4487 challenge virus available, we used the HA protein from the highly homologous influenza A/H1N1/California/04/2009 strain, which has a difference of only 2 amino acids. In all animals, the sera collected postinfection (solid lines) were able to induce CD107a expression on NK cells, while sera collected preinfection (dotted lines) did not show any activity (Fig. 7A and B). The ADCC-enhancing capacity was quantified by testing sera over a dilution range. There was no significant difference between the low- and high-dose groups in terms of EC_{50}s (Fig. 7C). However, similar to the binding antibody and virus NAb titers, the ADCC EC_{50}s were positively correlated with the cumulative virus load (Fig. 7D). A subset of CD107a-expressing cells, induced by

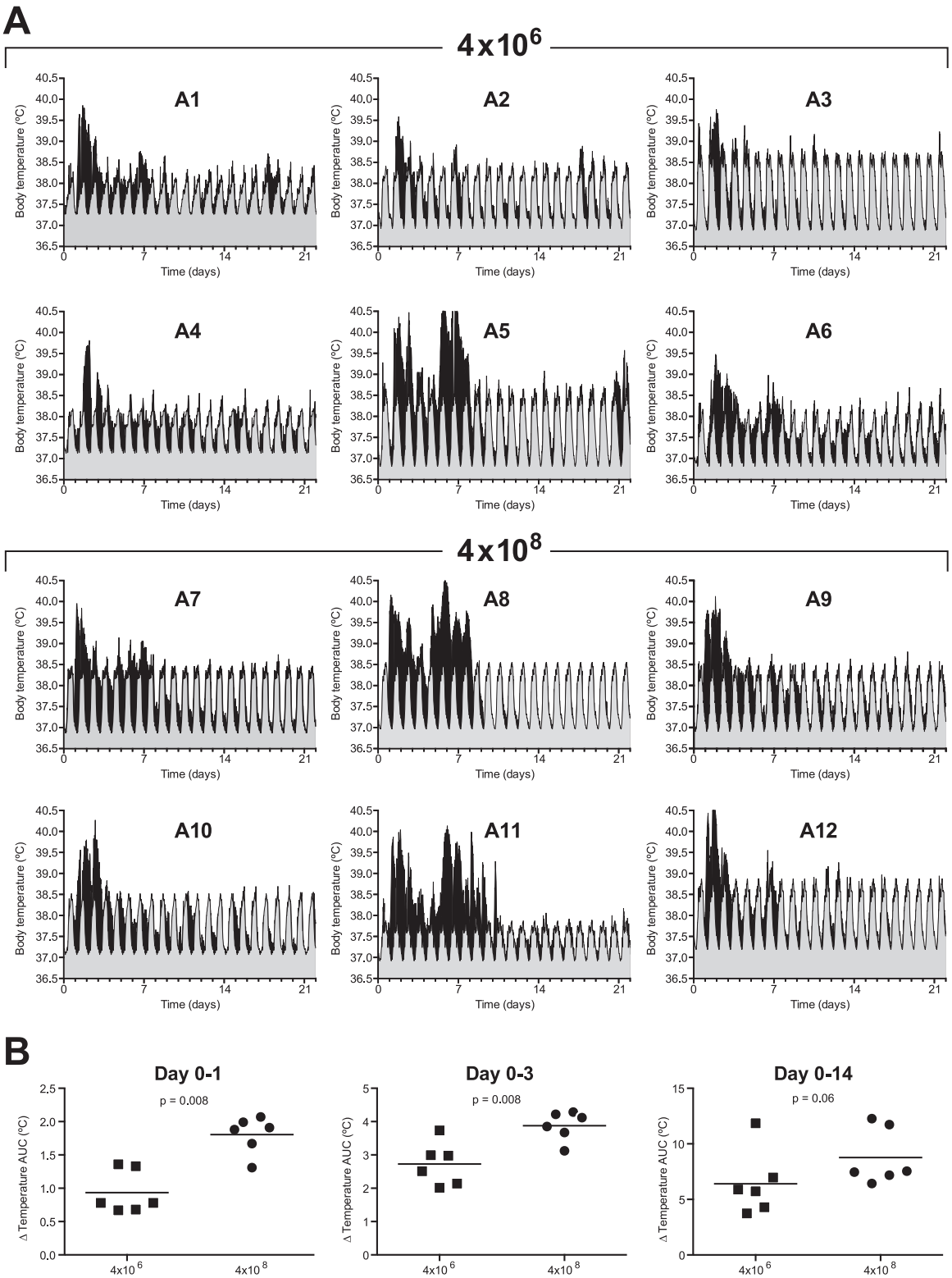

FIG 2 Body temperature of individual animals after low- and high-dose Mex4487 influenza virus inoculation. (A) Shown in black is the actually recorded temperature over time after infection for each individual animal. These temperatures are plotted on top of the circadian temperature pattern recorded before infection (gray area). The circadian pattern was calculated from the temperatures recorded during 3 weeks before infection. Gray areas represent the mean temperatures with the 95% confidence intervals. Animals 1 to 6 (A1 to A6) received a low-dose challenge (4×10^6 $TCID_{50}$), and animals 7 to 12 (A7 to A12) received a high-dose challenge (4×10^8 $TCID_{50}$). (B) Cumulative temperature increase, calculated as the AUC from the actually recorded temperature after infection, minus the mean circadian temperature pattern and the upper level of the 95% confidence interval recorded before infection during 1 day, 3 days, or 14 days after infection. Squares represent animals 1 to 6 (4×10^6 $TCID_{50}$), and circles represent animals 7 to 12 (4×10^8 $TCID_{50}$). Statistical differences between groups were determined with the Mann-Whitney test.

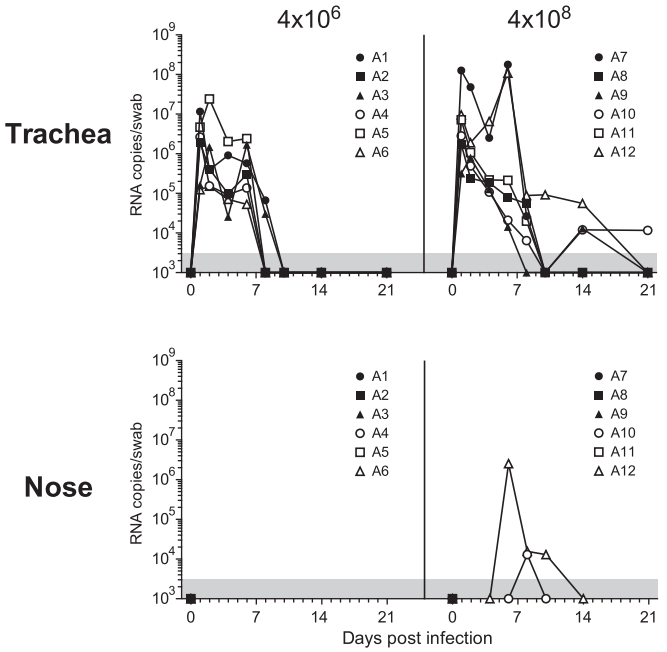

FIG 3 Virus replication in throat and nose swabs after low- and high-dose Mex4487 influenza virus inoculation. The virus loads, measured by RT-PCR in tracheal swabs and nose swabs, over time are shown. A1 to A12, animals 1 to 12. Gray areas at the bottom of the graphs indicate the lower limit of detection of the assay (3,162 RNA copies/ml).

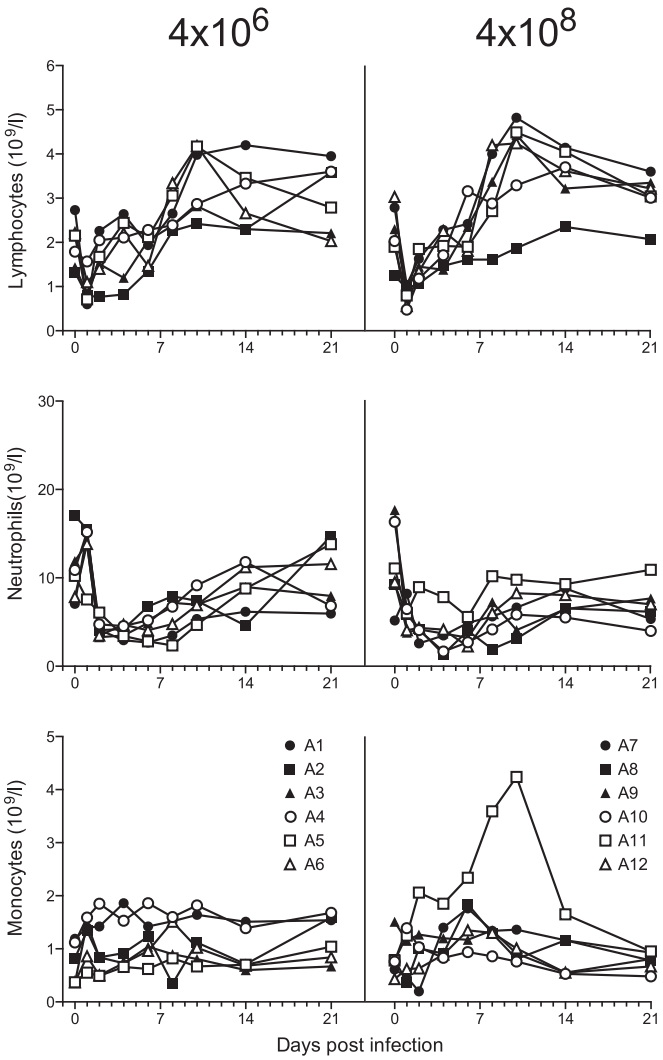

FIG 4 Lymphocyte, neutrophil, and monocyte counts in blood of cynomolgus macaques after low- and high-dose Mex4487 influenza virus inoculation. Shown are the absolute counts (per 10^9 cells per liter of whole blood) for each individual animal over time postinfection with Mex4487 influenza virus at day 0. A1 to A12, animals 1 to 12.

incubation with postinfection sera, also showed IFN-γ expression (Fig. 7E and F). However, IFN-γ was only observed on 1 to 5% of the NK cells, and although the percentage of positive cells decreased when sera were diluted, there was no sigmoid dilution curve, and EC_{50}s could not be calculated. CD107 expression on NK cells was also induced when postinfection sera were tested against the HA subunit of the heterologous influenza A Puerto Rico/8/34 strain (Fig. 7G and H). However, even at a 1:10 dilution, a plateau level was not reached, and EC_{50}s could not be calculated. Nonetheless, the serum dilution at which the curves for CD107a induction started to increase above baseline was about 100 to 300 times higher for the Puerto Rico/8/34 virus than for the California/04/2009 influenza virus strain for all animals, with the exception of animal 9. Hence, although there is substantial cross-recognition, the strain homologous to the challenge strain was recognized best.

DISCUSSION

In this study, we evaluated the effects of a standard-dose and high-dose influenza virus inoculation administered intrabronchially in cynomolgus macaques in an attempt to develop a more robust and uniform challenge model, potentially increasing the frequency and severity of clinical manifestations in the majority of the animals, such as sneezing and coughing, thereby spreading the virus to the upper respiratory tract. This would facilitate the evaluation of vaccine efficacy, reducing the number of animals needed per group, but risk the possibility of making the model too stringent to show protection of infection. Unfortunately, a 100-fold-higher influenza virus dose did not result in a significant increase in clinical symptoms in the majority of the animals or in terms of virus production in the trachea or nasal cavities. However, animals that received the high-dose inoculation developed more fever, a more rapid decrease in granulocyte counts in the blood, and a higher peak in IFN-γ production in serum at day 1 after infection. Induction of virus-specific ELISA Ab titers, virus neutralization titers, HAI titers, and ADCC EC_{50}s were not significantly different between the groups at 8 weeks postinfection. However, Ab binding, virus neutralization, and HAI titers and also ADCC EC_{50}s were positively correlated with total virus production in the trachea, implying a quantitative relationship between initial virus replication and immune induction measured later. ADCC activity was also detected against the distantly related influenza A/PR/8/34 (H1N1) strain, with an HA globular domain containing 76/328 different amino acids compared to Ca04, whereas there was no serum-neutralizing activity detected against this strain.

Evaluation of different doses for viral inoculation has been described for mice, ferrets, and occasionally in humans, but not yet for nonhuman primates (5–10, 17–21). These studies were

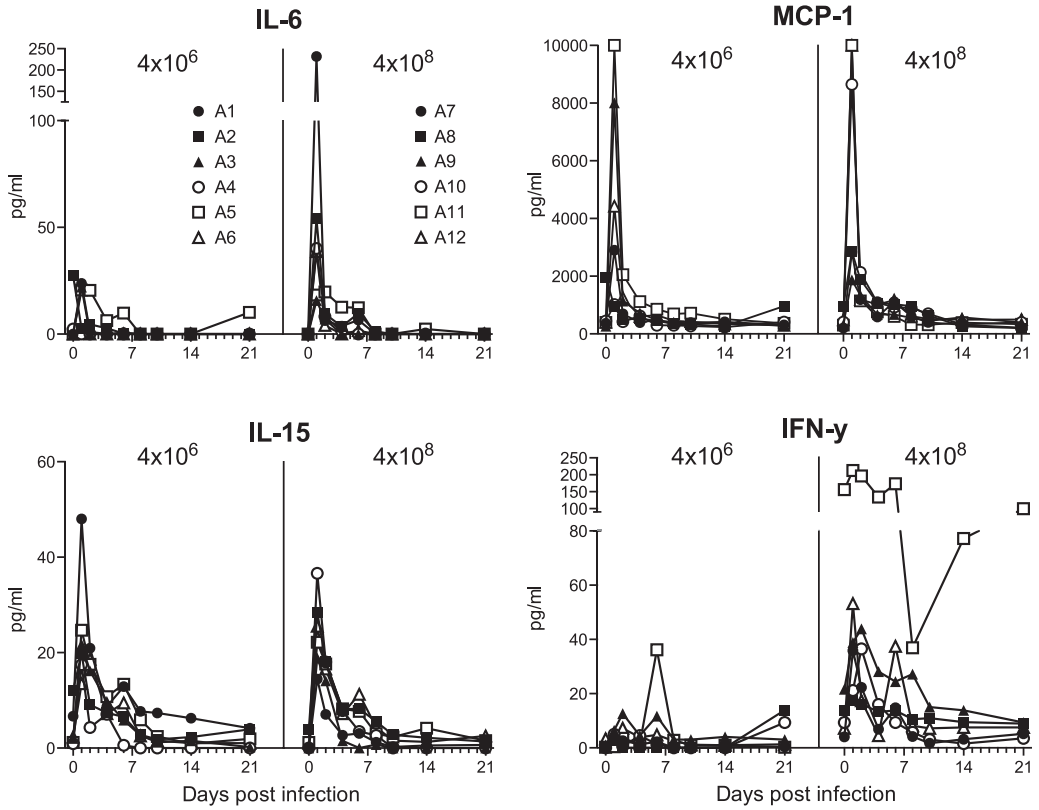

FIG 5 Cytokine and chemokine expression levels in serum of cynomolgus macaques after low- and high-dose Mex4487 influenza virus inoculation. Shown are the amounts of IL-6, MCP-1, IL-15, and IFN-γ (in picograms per milliliter) in serum, for each individual animal, at each time point. A1 to A12, animals 1 to 12.

either directed at finding the minimal infectious dose or minimal lethal dose or, in case of evaluation of attenuated viruses in humans, at finding the dose that resulted in adequate levels of infection while limiting development of clinical symptoms and fever. While we have seen no increase in clinical symptoms in the high-dose challenge group, other studies performed in ferrets and humans have shown increasing illness at a high virus inoculation dose (17–21). In agreement with these previous reports in humans (17, 19–21), we did observe more fever in the high-dose challenge group. The lack of clinical symptoms in our study may be related to the intrabronchial inoculation used by us, which is in contrast to the combined inoculation route in other animal studies (28) or the intranasal application used in most human studies. However, also in humans infected with pathogenic influenza virus, clinical manifestations may vary from asymptomatic to severe pneumonia (34). We previously reported that although the intrabronchial inoculation does result in lung pathology and virus production in the trachea and fever, virus replication in the nasal cavity is low, and sneezing, nasal discharge, or coughing are almost never seen (29), limiting dissemination of the virus to the upper respiratory tract. It could be argued that the intrabronchial infection is not the most representative for the human situation. However, the natural route of infection is still under debate and, as discussed by Killingley et al. (23), antiviral prophylaxis studies indicate that the pharynx and tracheo-bronchial tree are key sites for virus acquisition.

In agreement with previously published results (28, 29), we observed an increase in IL-6, MCP-1, and IL-15 in the blood, peaking at day 1 after infection. While MCP-1 and IL-15 were induced at similar levels in the low- and high-dose groups, IL-6 tended to be somewhat higher in the high-dose group, although statistical significance was not reached ($P = 0.06$). In addition, we observed a peak in IFN-γ production at day 1 after infection, which was significantly higher in the high-dose group. This early induction could be related to an early triggering of Th1 cells or NK cells, in agreement with their rapid depletion from the blood (Fig. 5 and data not shown). Triggering of NK cells may have been induced via binding of the influenza virus HA subunit to NKp46 (35). However, since IL-12 was not increased (data not shown), it is not clear how these cells might have been stimulated to produce IFN-γ.

Neutrophils were decreased after infection (Fig. 4), as reported previously (29, 36). However, the decrease was faster in the high-dose group, and the neutrophil blood count was negatively correlated with temperature increase during the first 3 days after infection (data not shown). Possibly the high virus dose induces more local tissue damage, resulting in enhanced migration of granulocytes from the blood to the lung. Enhanced granulocyte activation may subsequently have led to a higher fever.

All animals in the low-dose as well as high-dose group became virus positive in the trachea, and although virus production was higher in 2 out of 6 animals between days 1 and 6 after infection and was detected for a longer period in 3 out of 6 animals in the high-dose group, there was no significant difference in total virus production between the dose groups. A relation between inoculation dose and virus replication in nasal washes has been reported

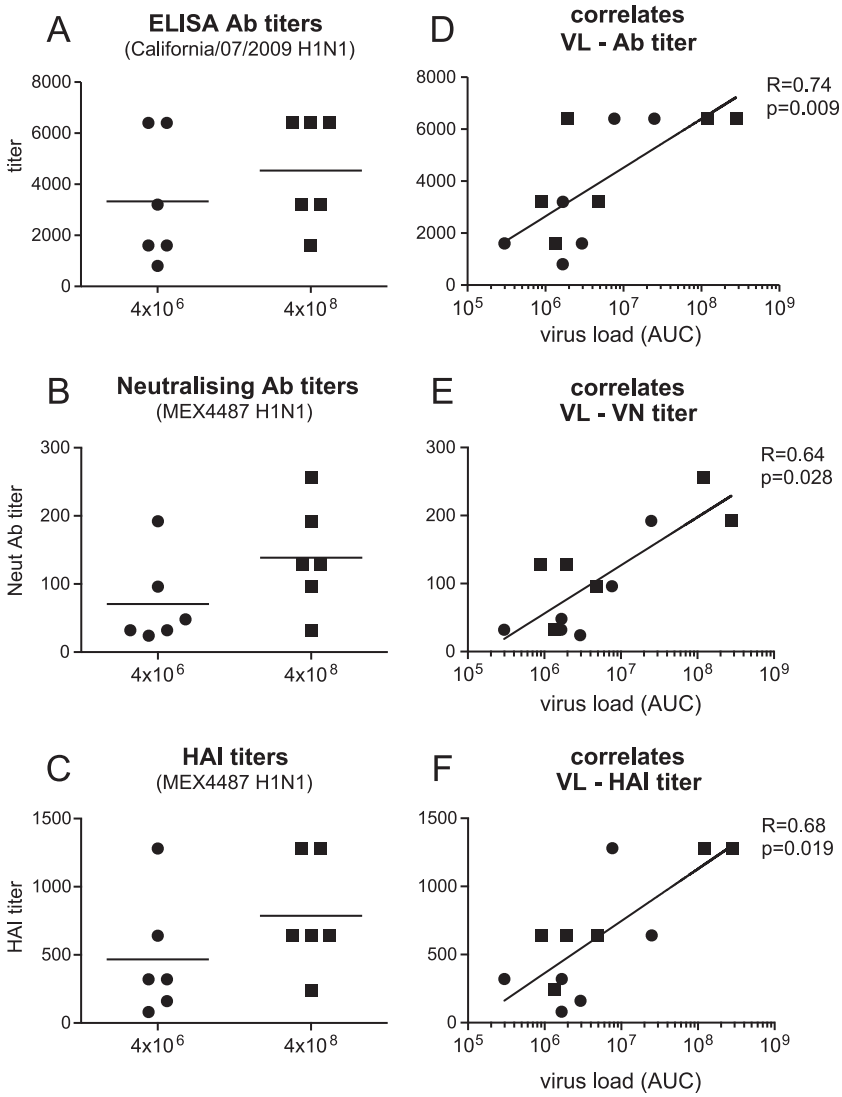

FIG 6 Antibody responses in serum of cynomolgus macaques after low- or high-dose Mex4487 influenza virus inoculation. Antibody responses were determined in serum collected 8 weeks after infection. Results are depicted either as a comparison between the low-dose (4×10^6 $TCID_{50}$; circles) and high-dose (4×10^8 $TCID_{50}$; squares) challenge groups (A to C) or are plotted against the cumulative virus load in the tracheal swabs (D to F). (A) ELISA antibody titers measured against the influenza A/California/07/2009 H1N1 HA subunit. (B) Neutralizing antibody titers measured against the Mex4487 challenge strain. (C) HAI titers measured against the Mex4487 challenge virus. (D to F) ELISA antibody titer, neutralizing antibody titer, and HAI titer plotted against cumulative virus load in the tracheal swabs. Cumulative virus load was calculated for each animal as the AUC for the virus load, measured via RT-PCR in tracheal swabs (depicted in Fig. 2). Statistical analysis of differences between the low- and high-dose challenge groups was performed with the Mann-Whitney test. Correlation with virus load was calculated with the Spearman correlation test. The black line represents interpolated data, as a semilog standard curve.

in several human studies (17, 18, 21), but other studies have shown no relation (19, 20). Also, in ferrets conflicting results on the relation between virus inoculation dose and levels of virus replication have been reported (6, 8–10).

Few studies have addressed the induction of immune responses in relation to virus inoculation dose or virus replication, and these studies have yielded conflicting results (10, 18–20). We observed a positive correlation between total virus production in the trachea and induction of Ab binding titers, neutralizing antibody and HAI titers, and ADCC EC_{50}s directed against influenza A virus Mex4487 or closely related strains. These data provide a clear indication that induction of an effective humoral immune response against the virus is directly related to the level of virus replication achieved. In agreement with recently published results showing that ADCC is associated with control of pandemic H1N1 influenza virus infection in macaques (37), we observed that infection with pH1N1 influenza virus resulted in induction of ADCC antibodies against the HA subunit. Furthermore, while virus neutralization was only seen against the homologous pH1N1 Mex487 virus and not against a distantly related influenza A/PR/8/34 H1N1 virus, ADCC activity was more cross-reactive, since both viruses were recognized. However, it must be noted that ADCC was observed at 100- to 300-fold-lower serum virus concentrations against the homologous Mex4487 strain than with the PR/8/34 strain. Titers of functional antibodies, including virus-neutralizing, HAI, and ADCC-inducing antibodies, were posi-

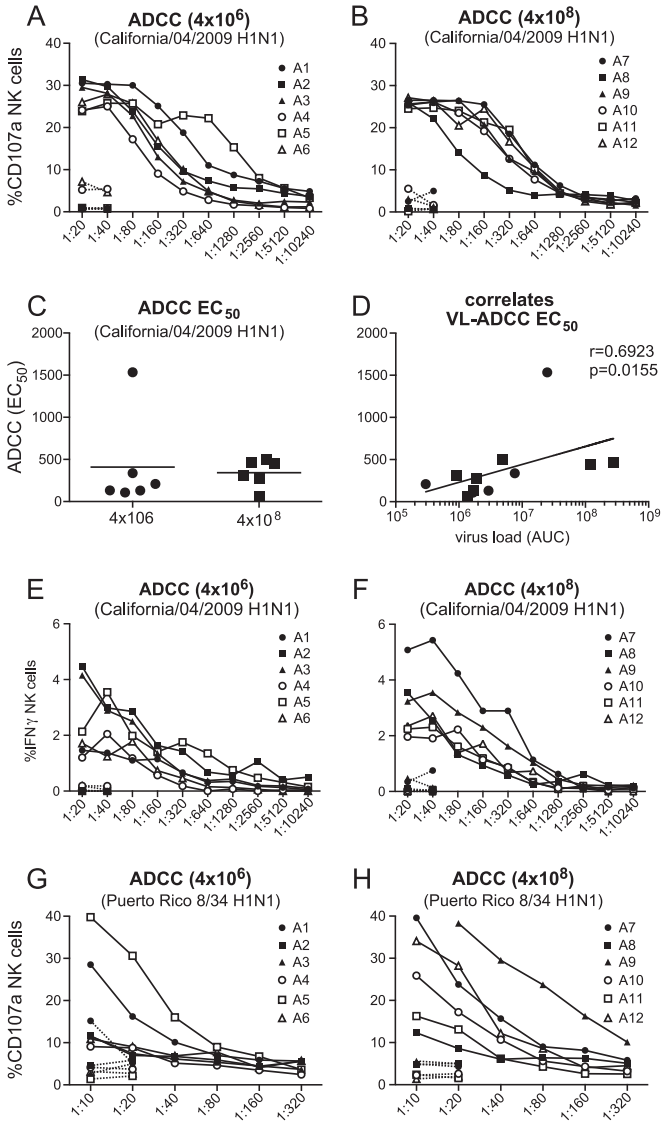

FIG 7 ADCC measured in serum of cynomolgus macaques after low- or high-dose Mex4487 influenza virus inoculation. The graphs show induction of CD107a IFN-γ expression in NK cells after incubation on HA-coated plates in the presence of different dilutions of serum collected before (dotted lines) or 8 weeks after (solid lines) virus inoculation. (A and B) Percentages of NK cells expressing CD107a after incubation with serum from animals in the low-dose (4×10^6 $TCID_{50}$) and high-dose (4×10^8 $TCID_{50}$) groups, respectively, measured on wells coated with HA from influenza A California/04/2009. (C and D) EC_{50}s in the low- versus high-dose group (C) and EC_{50}s plotted against cumulative virus load (AUC) in tracheal swabs, measured on wells coated with HA from influenza virus A California/04/2009 (D). Filled circles are results for the low-dose group, and filled squares are results for the high-dose group animals. (E and F) Percentage of NK cells expressing IFN-γ after incubation with serum from animals in the low-dose (4×10^6 $TCID_{50}$) (E) and high-dose (4×10^8 $TCID_{50}$) (F) groups, measured on wells coated with HA from influenza A California/04/2009. (G and H) Percentage of NK cells expressing CD107a after incubation with serum from animals in the low-dose (4×10^6 $TCID_{50}$) and high-dose (4×10^8 $TCID_{50}$) groups, measured on wells coated with HA from influenza virus A/Puerto Rico/8/34. A1 to A12, animals 1 to 12. Correlation with virus load was calculated by using the Spearman correlation test. The black line represents interpolated data, as a semilog standard curve.

tively correlated with the level of total pH1N1 virus binding antibody titers. Hence, it appears that induction of a higher total virus-specific antibody response translates into a similar increase in induction of functional antibodies, and these may form a relatively constant fraction of the total response.

Our studies have shown that a 100-fold-higher virus inoculation dose does not necessarily translate to increased virus production and clinical symptoms and that the previously applied dose range of 10^6 to 10^7 $TCID_{50}$ appears adequate for this model. The correlation between amount of virus produced and induction of functional antibody responses against the virus and mutual relationship between total antibody response and induction of functional antibodies may provide a basis for analyzing vaccine effectiveness in relation to natural infection in humans. For instance, Jegaskanda has already demonstrated that ADCC is associated with control of pandemic H1N1 influenza virus infection in macaques (37), but ADCC antibodies were not induced following standard trivalent influenza virus protein vaccination (25). These data may also be relevant in view of the discussion of appropriate correlates of protection, identifying which immune responses are responsible for viral clearance. Ideally, these responses will have to be induced by vaccination and may therefore be relevant for criteria used for licensing by the European Union (38) and the United States (33, 39–44).

ACKNOWLEDGMENTS

This study was sponsored by Crucell Holland B.V., Janssen Pharmaceutical Companies of Johnson & Johnson, and an institutional subsidy from the BPRC.

We thank Y. Li and G. Kobinger from the Public Health Agency of Canada, National Microbiology Laboratory, Canadian Science Centre for Human and Animal Health, Winnipeg, MB, Canada, for providing the influenza A/Mexico/InDRE4487/2009 (H1N1) (Mex4487) virus. We thank J. de Jonge (National Institute of Public Health and the Environment [RIVM], Bilthoven, The Netherlands) and H. Feldmann (NIH, Hamilton, MT, USA) for expert advice and H. van Westbroek for preparing the figures.

FUNDING INFORMATION

This study was sponsored by Crucell Holland B.V., Janssen Pharmaceutical Companies of Johnson & Johnson, and an institutional subsidy from the BPRC.

REFERENCES

1. **Bouvier NM, Lowen AC.** 2010. Animal models for influenza virus pathogenesis and transmission. Viruses **2:**1530–1563. http://dx.doi.org/10.3390/v20801530.
2. **Davis AS, Taubenberger JK, Bray M.** 2015. The use of nonhuman primates in research on seasonal, pandemic and avian influenza, 1893-2014. Antiviral Res **117:**75–98. http://dx.doi.org/10.1016/j.antiviral.2015.02.011.
3. **Bodewes R, Rimmelzwaan GF, Osterhaus AD.** 2010. Animal models for the preclinical evaluation of candidate influenza vaccines. Expert Rev Vaccines **9:**59–72. http://dx.doi.org/10.1586/erv.09.148.
4. **Lednicky JA, Croutch CR, Lawrence SJ, Hamilton SB, Daniels DE, Astroff B.** 2010. A nonlethal young domesticated ferret (Mustela putorius furo) model for studying pandemic influenza virus A/California/04/2009 (H1N1). Comp Med **60:**364–368.
5. **Dimmock NJ, Marriott AC.** 2006. In vivo antiviral activity: defective interfering virus protects better against virulent influenza A virus than avirulent virus. J Gen Virol **87:**1259–1265. http://dx.doi.org/10.1099/vir.0.81678-0.
6. **Gustin KM, Belser JA, Wadford DA, Pearce MB, Katz JM, Tumpey TM, Maines TR.** 2011. Influenza virus aerosol exposure and analytical system

for ferrets. Proc Natl Acad Sci U S A **108:**8432–8437. http://dx.doi.org/10.1073/pnas.1100768108.
7. **Kiso M, Ozawa M, Le MT, Imai H, Takahashi K, Kakugawa S, Noda T, Horimoto T, Kawaoka Y.** 2011. Effect of an asparagine-to-serine mutation at position 294 in neuraminidase on the pathogenicity of highly pathogenic H5N1 influenza A virus. J Virol **85:**4667–4672. http://dx.doi.org/10.1128/JVI.00047-11.
8. **MacInnes H, Zhou Y, Gouveia K, Cromwell J, Lowery K, Layton RC, Zubelewicz M, Sampath R, Hofstadler S, Liu Y, Cheng YS, Koster F.** 2011. Transmission of aerosolized seasonal H1N1 influenza A to ferrets. PLoS One **6:**e24448. http://dx.doi.org/10.1371/journal.pone.0024448.
9. **Marriott AC, Dove BK, Whittaker CJ, Bruce C, Ryan KA, Bean TJ, Rayner E, Pearson G, Taylor I, Dowall S, Plank J, Newman E, Barclay WS, Dimmock NJ, Easton AJ, Hallis B, Silman NJ, Carroll MW.** 2014. Low dose influenza virus challenge in the ferret leads to increased virus shedding and greater sensitivity to oseltamivir. PLoS One **9:**e94090. http://dx.doi.org/10.1371/journal.pone.0094090.
10. **McBrayer A, Camp JV, Tapp R, Yamshchikov V, Grimes S, Noah DL, Jonsson CB, Bruder CE.** 2010. Course of seasonal influenza A/Brisbane/59/07 H1N1 infection in the ferret. Virol J **7:**149. http://dx.doi.org/10.1186/1743-422X-7-149.
11. **van den Brand JM, Stittelaar KJ, van Amerongen G, Rimmelzwaan GF, Simon J, de Wit E, Munster V, Bestebroer T, Fouchier RA, Kuiken T, Osterhaus AD.** 2010. Severity of pneumonia due to new H1N1 influenza virus in ferrets is intermediate between that due to seasonal H1N1 virus and highly pathogenic avian influenza H5N1 virus. J Infect Dis **201:**993–999. http://dx.doi.org/10.1086/651132.
12. **Fan S, Gao Y, Shinya K, Li CK, Li Y, Shi J, Jiang Y, Suo Y, Tong T, Zhong G, Song J, Zhang Y, Tian G, Guan Y, Xu XN, Bu Z, Kawaoka Y, Chen H.** 2009. Immunogenicity and protective efficacy of a live attenuated H5N1 vaccine in nonhuman primates. PLoS Pathog **5:**e1000409. http://dx.doi.org/10.1371/journal.ppat.1000409.
13. **Kreijtz JH, Suezer Y, de Mutsert G, van den Brand JM, van Amerongen G, Schnierle BS, Kuiken T, Fouchier RA, Lower J, Osterhaus AD, Sutter G, Rimmelzwaan GF.** 2009. Recombinant modified vaccinia virus Ankara expressing the hemagglutinin gene confers protection against homologous and heterologous H5N1 influenza virus infections in macaques. J Infect Dis **199:**405–413. http://dx.doi.org/10.1086/595984.
14. **Laddy DJ, Yan J, Khan AS, Andersen H, Cohn A, Greenhouse J, Lewis M, Manischewitz J, King LR, Golding H, Draghia-Akli R, Weiner DB.** 2009. Electroporation of synthetic DNA antigens offers protection in nonhuman primates challenged with highly pathogenic avian influenza virus. J Virol **83:**4624–4630. http://dx.doi.org/10.1128/JVI.02335-08.
15. **Rimmelzwaan GF, Baars M, van Amerongen G, van Beek R, Osterhaus AD.** 2001. A single dose of an ISCOM influenza vaccine induces long-lasting protective immunity against homologous challenge infection but fails to protect cynomolgus macaques against distant drift variants of influenza A (H3N2) viruses. Vaccine **20:**158–163. http://dx.doi.org/10.1016/S0264-410X(01)00262-6.
16. **Carrat F, Vergu E, Ferguson NM, Lemaitre M, Cauchemez S, Leach S, Valleron AJ.** 2008. Time lines of infection and disease in human influenza: a review of volunteer challenge studies. Am J Epidemiol **167:**775–785. http://dx.doi.org/10.1093/aje/kwm375.
17. **Clements ML, O'Donnell S, Levine MM, Chanock RM, Murphy BR.** 1983. Dose response of A/Alaska/6/77 (H3N2) cold-adapted reassortant vaccine virus in adult volunteers: role of local antibody in resistance to infection with vaccine virus. Infect Immun **40:**1044–1051.
18. **Keitel WA, Couch RB, Cate TR, Six HR, Baxter BD.** 1990. Cold recombinant influenza B/Texas/1/84 vaccine virus (CRB 87): attenuation, immunogenicity, and efficacy against homotypic challenge. J Infect Dis **161:**22–26. http://dx.doi.org/10.1093/infdis/161.1.22.
19. **Murphy BR, Holley HP, Jr, Berquist EJ, Levine MM, Spring SB, Maassab HF, Kendal AP, Chanock RM.** 1979. Cold-adapted variants of influenza A virus: evaluation in adult seronegative volunteers of A/Scotland/840/74 and A/Victoria/3/75 cold-adapted recombinants derived from the cold-adapted A/Ann Arbor/6/60 strain. Infect Immun **23:**253–259.
20. **Murphy BR, Rennels MB, Douglas RG, Jr, Betts RF, Couch RB, Cate TR, Jr, Chanock RM, Kendal AP, Maassab HF, Suwanagool S, Sotman SB, Cisneros LA, Anthony WC, Nalin DR, Levine MM.** 1980. Evaluation of influenza A/Hong Kong/123/77 (H1N1) ts-1A2 and cold-adapted recombinant viruses in seronegative adult volunteers. Infect Immun **29:**348–355.
21. **Sears SD, Clements ML, Betts RF, Maassab HF, Murphy BR, Snyder MH.** 1988. Comparison of live, attenuated H1N1 and H3N2 cold-adapted and avian-human influenza A reassortant viruses and inactivated virus vaccine in adults. J Infect Dis **158:**1209–1219. http://dx.doi.org/10.1093/infdis/158.6.1209.
22. **Alford RH, Kasel JA, Gerone PJ, Knight V.** 1966. Human influenza resulting from aerosol inhalation. Proc Soc Exp Biol Med **122:**800–804. http://dx.doi.org/10.3181/00379727-122-31255.
23. **Killingley B, Enstone J, Booy R, Hayward A, Oxford J, Ferguson N, Nguyen Van-Tam J, Influenza Transmission Strategy Development Group.** 2011. Potential role of human challenge studies for investigation of influenza transmission. Lancet Infect Dis **11:**879–886. http://dx.doi.org/10.1016/S1473-3099(11)70142-6.
24. **Weinfurter JT, Brunner K, Capuano SV, III, Li C, Broman KW, Kawaoka Y, Friedrich TC.** 2011. Cross-reactive T cells are involved in rapid clearance of 2009 pandemic H1N1 influenza virus in nonhuman primates. PLoS Pathog **7:**e1002381. http://dx.doi.org/10.1371/journal.ppat.1002381.
25. **Jegaskanda S, Amarasena TH, Laurie KL, Tan HX, Butler J, Parsons MS, Alcantara S, Petravic J, Davenport MP, Hurt AC, Reading PC, Kent SJ.** 2013. Standard trivalent influenza virus protein vaccination does not prime antibody-dependent cellular cytotoxicity in macaques. J Virol **87:**13706–13718. http://dx.doi.org/10.1128/JVI.01666-13.
26. **Josset L, Engelmann F, Haberthur K, Kelly S, Park B, Kawoaka Y, Garcia-Sastre A, Katze MG, Messaoudi I.** 2012. Increased viral loads and exacerbated innate host responses in aged macaques infected with the 2009 pandemic H1N1 influenza A virus. J Virol **86:**11115–11127. http://dx.doi.org/10.1128/JVI.01571-12.
27. **Brining DL, Mattoon JS, Kercher L, LaCasse RA, Safronetz D, Feldmann H, Parnell MJ.** 2010. Thoracic radiography as a refinement methodology for the study of H1N1 influenza in cynomologus macaques (Macaca fascicularis). Comp Med **60:**389–395.
28. **Safronetz D, Rockx B, Feldmann F, Belisle SE, Palermo RE, Brining D, Gardner D, Proll SC, Marzi A, Tsuda Y, Lacasse RA, Kercher L, York A, Korth MJ, Long D, Rosenke R, Shupert WL, Aranda CA, Mattoon JS, Kobasa D, Kobinger G, Li Y, Taubenberger JK, Richt JA, Parnell M, Ebihara H, Kawaoka Y, Katze MG, Feldmann H.** 2011. Pandemic swine-origin H1N1 influenza A virus isolates show heterogeneous virulence in macaques. J Virol **85:**1214–1223. http://dx.doi.org/10.1128/JVI.01848-10.
29. **Mooij P, Koopman G, Mortier D, van Heteren M, Oostermeijer H, Fagrouch Z, de Laat R, Kobinger G, Li Y, Remarque EJ, Kondova I, Verschoor EJ, Bogers WM.** 2015. Pandemic swine-origin H1N1 influenza virus replicates to higher levels and induces more fever and acute inflammatory cytokines in cynomolgus versus rhesus monkeys and can replicate in common marmosets. PLoS One **10:**e0126132. http://dx.doi.org/10.1371/journal.pone.0126132.
30. **Van Wesenbeeck L, Meeuws H, Van Immerseel A, Ispas G, Schmidt K, Houspie L, Van Ranst M, Stuyver L.** 2013. Comparison of the FilmArray RP, Verigene RV+, and Prodesse ProFLU+/FAST+ multiplex platforms for detection of influenza viruses in clinical samples from the 2011-2012 influenza season in Belgium. J Clin Microbiol **51:**2977–2985. http://dx.doi.org/10.1128/JCM.00911-13.
31. **Mahdi Abdel Hamid M, Remarque EJ, van Duivenvoorde LM, van der Werff N, Walraven V, Faber BW, Kocken CH, Thomas AW.** 2011. Vaccination with Plasmodium knowlesi AMA1 formulated in the novel adjuvant co-vaccine HT protects against blood-stage challenge in rhesus macaques. PLoS One **6:**e20547. http://dx.doi.org/10.1371/journal.pone.0020547.
32. **World Health Organization.** 2002. WHO manual on animal influenza diagnosis and surveillance. WHO Department of Communicable Disease Surveillance and Response, Geneva, Switzerland.
33. **Jegaskanda S, Job ER, Kramski M, Laurie K, Isitman G, de Rose R, Winnall WR, Stratov I, Brooks AG, Reading PC, Kent SJ.** 2013. Cross-reactive influenza-specific antibody-dependent cellular cytotoxicity antibodies in the absence of neutralizing antibodies. J Immunol **190:**1837–1848. http://dx.doi.org/10.4049/jimmunol.1201574.
34. **Chen Z, Liu H, Lu J, Luo L, Li K, Liu Y, Lau EH, Di B, Wang H, Yang Z, Xiao X.** 2014. Asymptomatic, mild, and severe influenza A(H7N9) virus infection in humans, Guangzhou, China. Emerg Infect Dis **20:**1535–1540. http://dx.doi.org/10.3201/eid2009.140424.
35. **Jost S, Altfeld M.** 2013. Control of human viral infections by natural killer

cells. Annu Rev Immunol **31:**163–194. http://dx.doi.org/10.1146/annurev-immunol-032712-100001.

36. **Baskin CR, Bielefeldt-Ohmann H, Tumpey TM, Sabourin PJ, Long JP, Garcia-Sastre A, Tolnay AE, Albrecht R, Pyles JA, Olson PH, Aicher LD, Rosenzweig ER, Murali-Krishna K, Clark EA, Kotur MS, Fornek JL, Proll S, Palermo RE, Sabourin CL, Katze MG.** 2009. Early and sustained innate immune response defines pathology and death in nonhuman primates infected by highly pathogenic influenza virus. Proc Natl Acad Sci U S A **106:**3455–3460. http://dx.doi.org/10.1073/pnas.0813234106.
37. **Jegaskanda S, Weinfurter JT, Friedrich TC, Kent SJ.** 2013. Antibody-dependent cellular cytotoxicity is associated with control of pandemic H1N1 influenza virus infection of macaques. J Virol **87:**5512–5522. http://dx.doi.org/10.1128/JVI.03030-12.
38. **European Medicines Agency.** 1996. Note for guidance on harmonisation or requirements for influenza vaccines. The European Agency for the Evaluation of Medicinal Products, London, England.
39. **CDC.** 2006. Prevention and control of influenza. Recommendations of the Advisory Committee on Immunization Practices (ACIP). MMRW Recommend Rep **55**(RR10):1–42. http://www.cdc.gov/MMWR/preview/mmwrhtml/rr5510a1.htm.
40. **Black S, Nicolay U, Vesikari T, Knuf M, Del Giudice G, Della Cioppa G, Tsai T, Clemens R, Rappuoli R.** 2011. Hemagglutination inhibition antibody titers as a correlate of protection for inactivated influenza vaccines in children. Pediatr Infect Dis J **30:**1081–1085. http://dx.doi.org/10.1097/INF.0b013e3182367662.
41. **Lee MS, Mahmood K, Adhikary L, August MJ, Cordova J, Cho I, Kemble G, Reisinger K, Walker RE, Mendelman PM.** 2004. Measuring antibody responses to a live attenuated influenza vaccine in children. Pediatr Infect Dis J **23:**852–856. http://dx.doi.org/10.1097/01.inf.0000137566.87691.3b.
42. **Leroux-Roels I, Leroux-Roels G.** 2009. Current status and progress of prepandemic and pandemic influenza vaccine development. Expert Rev Vaccines **8:**401–423. http://dx.doi.org/10.1586/erv.09.15.
43. **Sridhar S, Begom S, Bermingham A, Hoschler K, Adamson W, Carman W, Bean T, Barclay W, Deeks JJ, Lalvani A.** 2013. Cellular immune correlates of protection against symptomatic pandemic influenza. Nat Med **19:**1305–1312. http://dx.doi.org/10.1038/nm.3350.
44. **Wilkinson TM, Li CK, Chui CS, Huang AK, Perkins M, Liebner JC, Lambkin-Williams R, Gilbert A, Oxford J, Nicholas B, Staples KJ, Dong T, Douek DC, McMichael AJ, Xu XN.** 2012. Preexisting influenza-specific CD4+ T cells correlate with disease protection against influenza challenge in humans. Nat Med **18:**274–280. http://dx.doi.org/10.1038/nm.2612.